Bulletin of Earthquake Engineering
https://doi.org/10.1007/s10518-023-01656-4

S.I. : NATECH RISK ASSESSMENT OF HAZARDOUS FACILITIES

Acceleration-sensitive ancillary elements in industrial facilities: alternative seismic design approaches in the new Eurocode

A. K. Kazantzi[1,2] · N. D. Karaferis[3] · V. E. Melissianos[3] · D. Vamvatsikos[2,3]

Received: 1 November 2022 / Accepted: 18 February 2023

Abstract
The Eurocode 8—Part 4 approaches, per their December 2022 update, are presented for the design of acceleration-sensitive industrial ancillary components. The seismic performance of such nested and/or supported ancillary elements, namely mechanical and electrical equipment, machinery, vessels, etc. is critical for the safety and operability of an industrial facility in the aftermath of an earthquake. Of primary importance are the structural characteristics of the supporting structure and the supported component, pertaining to resonance, strength, and ductility, and whether these are known (and to what degree) during initial design and/or subsequent modifications and upgrades. Depending on the availability and reliability of information on the overall system, the Eurocode methods comprise (a) a detailed component/structure-specific design accounting for all pertinent component and building characteristics, equivalent to typical building design per Eurocode 8—Part 1–2, (b) a conservative approach where a blanket safety factor is applied when little or no such data is available, and (c) a ductile design founded on the novel concept of inserting a fuse of verified ductility and strength in the load path between the supporting structure and the ancillary element. All three methods are evaluated and compared on the basis of a case-study industrial structure, showing how an engineer can achieve economy without compromising safety under different levels of uncertainty.

Keywords Ancillary elements · Industrial facilities · Eurocode · Design · Nonstructural components

✉ A. K. Kazantzi
kazantzi@ihu.gr

[1] Department of Civil Engineering, International Hellenic University, Serres, Greece

[2] Societal Resilience & Climate Change (SoReCC) Center of Excellence, Diegem, Belgium

[3] School of Civil Engineering, National Technical University of Athens, Athens, Greece

Published online: 21 March 2023

1 Introduction

Ancillary elements in industrial facilities, such as piping, heat exchangers, electrical/mechanical equipment, vessels, fire protection equipment etc., are by default special nonstructural components playing a decisive role in the safe and undisrupted operation of industrial plants. Such equipment are also referred to in recent literature by the terms of nonstructural components and nested equipment. We shall employ the three terms interchangeably in the following. Their contribution to the integrity of an entire facility is further stressed by the fact that the structures, supporting or nesting such components, are typically overdesigned, well-constructed, and routinely maintained. Hence, one may not expect such structures to sustain any substantial direct damages in case of a moderate or even a strong earthquake event. On the other hand, the equipment-supporting asset is likely to sustain indirect severe damages due to the inferior seismic performance of the nested ancillary elements (Pinkawa et al. 2022), potentially triggering a series of adverse cascading incidents (e.g., uncontrolled fires, explosions, release of toxic substances) that could affect their load-bearing structural elements, as well as the neighbouring assets and surrounding area, consequently resulting in a catastrophic failure.

Ancillary elements can be discretised into two main categories, according to the failure mode to which they are prone (FEMA, 2020): (a) drift-sensitive ones, referring to those components/anchorages that are likely to sustain damage due to excessive interstorey drift demands imposed to the supporting structure (e.g., piping spanning across the building height) or (b) acceleration-sensitive ones, which are prone to sustaining damage due to excessive acceleration demands (e.g., vessels, heat exchangers) developed in response to the floor/ground motion imposed at their base; a number of components can be also classified in both categories (Taghavi and Miranda 2003).

Excessive deformation or acceleration demands may result in damage to the equipment itself, for instance, due to the exceedance of the manufacturer acceleration limits that can be sustained by vibration-sensitive electromechanical components, such as electrical panels, switchboards, or even magnetic resonance imaging units (Gandelli et al. 2019); damage may also be localised to a component's anchorage system, for example due to the exceedance of the strength/ductility capacity of its brackets, plates and/or bolts that intervene between the equipment and its floor attachment(s). In general, when it comes to protecting the equipment versus its anchorage, reasons of cost and safety dictate that one would opt for the first, assuming anchorage damage is contained and does not otherwise transfer to the component itself, or even to primary structural elements of the supporting structure.

Safeguarding the seismic integrity of drift-sensitive ancillary equipment and their attachment points requires accounting for the deformation response of the supporting structure, while the equipment itself is assumed to conform to supporting-structure deformations. Contrarily, the design of acceleration-sensitive components and their anchorage system is more complex. This is due to the acceleration demands that are imposed at the component level, and eventually at the anchorage points, being highly dependent not only to the dynamic characteristics (i.e., period, damping, mode shapes) and the response (linear or nonlinear) of the supporting structure but also to the dynamic characteristics (i.e., natural period and damping) and the ductility of the nonstructural component, as well as to the location where it is attached, as documented by numerous studies, e.g., Peters et al. (1977); Singh (1980); Igusa and Der Kiureghian (1985); Adam and Fotiu (2000); Taghavi and Miranda (2003); Sankaranarayanan and Medina (2007); NIST (2017); Kazantzi et al. (2020a). It should be also noted that the supporting structure acts as a filtering medium,

essentially transforming the ground motion acceleration waveform to different narrow-band floor acceleration motions along the building height. Also, it has been shown that the ductility of the component defines extensively how much the floor acceleration is amplified at the component level. Therefore, one may conclude that designing acceleration-sensitive equipment is a non-trivial process since (a) it requires a great deal of information that substantially affects the outcome of the design process and (b) the designer rarely has a good level of knowledge on the needed input as well as access to pertinent reliable data, e.g., component period, supporting-structure ductility, anchorage ductility.

In general, the simplest approaches for the design of most acceleration-sensitive ancillary elements are founded on two common important assumptions: (a) the component mass is small relatively to the mass of the supporting structure, justifying not accounting for component-structure interaction, and (b) the supporting structural element(s) (e.g., the concrete slab) are stiff enough to avoid being affected by the vibrating components. If both conditions are satisfied, then one may decouple the problem by first analysing/designing the supporting structure and then using the resulting displacements/accelerations at the location of the ancillary component(s) or its anchorage point(s) to analyse/design the component (e.g., Merino Vela et al. 2019; Kazantzi et al. 2022a). As a remark, there are no universally-accepted mass and stiffness thresholds/criteria to define the applicability range of the aforementioned, so-called, cascade method (Lee and Chen 1975; Taghavi and Miranda 2008).

Even assuming that the aforementioned assumptions hold, a comprehensive and practicable design approach is still needed to ensure that the satisfactory seismic performance of the acceleration-sensitive ancillary elements is not undermined by designer choices under the uncertainties faced. It should be pointed out that such uncertainties may be reduced and the required safety level largely guaranteed by the utilisation of conventional or novel base-isolation devices (e.g., Wang et al. 2017). Such devices essentially decouple the motion of the acceleration-sensitive equipment from the motion of the supporting slab and protect the equipment from seismic-induced damage, provided that the capacity of the isolation system is not exceeded.

Alternatively, the anchorage/bracing system can be designed to remain elastic even at high seismic intensity levels. From a practical standpoint, this approach seems more cost-effective when compared to base-isolation devices, since the contribution of the anchorage/bracing system (e.g., brackets, braces, bolts, plates) to the capital cost of the building is minimal. In practice, increasing the section sizes and/or upgrading the material strength of the fasteners to guarantee an elastic seismic performance is rather inexpensive. Nevertheless, similarly to primary structural systems, an elastic seismic performance comes with the cost of higher accelerations for the component itself. Even worse, an elastic component can be subjected to extremely amplified accelerations due to resonance, which are only approximately accounted for in the design codes, since they can lead to excessive safety factors that are not easy to justify in practice.

An alternative design option can be founded on the ductile fuse concept proposed by Miranda et al. (2018) for acceleration-sensitive nonstructural elements. This aims at mitigating the imposed seismic forces by inserting an easily repairable or replaceable ductile fuse between the ancillary component and the supporting structure. The benefits of allowing the bracing/anchorage system of the nonstructural component to yield have been showcased in recent analytical and experimental studies (e.g., Kazantzi et al. 2020a, b, 2022b; Vukobratovic and Ruggieri 2021; Elkady et al. 2022). The common ground in the outcomes of these studies is that even a small provision of component ductility can substantially lower the resonant peak response caused by the narrow-band floor acceleration

spectra. Alternatively, this dissipative design concept can also be materialised, for instance, by allowing the component to slide or rock, two options that are theoretically sound, yet may introduce serviceability issues in connecting elements (e.g., piping, cables, etc.).

A typical industrial equipment-supporting building is considered in this study to present and evaluate the alternative design methods for ancillary elements offered in the latest revised version of Eurocode 8 (prEN 1998:2022), which at the time of writing (January 2023) is under public enquiry. The aim is to shed light onto these methods by revealing the impact of the underlying assumptions, as well as of the uncertainties emerging from the engineer's choices on the properties of the elements. The anchorage of the ancillary elements is designed via both non-dissipative and dissipative approaches. Especially for the latter, only the case of yielding ductile fuses is analytically investigated. The presented findings can be projected to other energy/deformation dissipation mechanisms, although not always in a trivial manner.

2 Design approaches

The design of nonstructural components per se, requires a great deal of knowledge on the vibration characteristics of the primary (supporting) structure, as well the secondary system (ancillary element) to attain an acceptably low risk level. In particular, the seismic ground acceleration that is imposed to the building base undergoes two modulations, which often involve amplitude amplification (see Fig. 1): (a) due to its dynamic filtering by the vibration modes of the supporting structure and (b) due to the flexibility

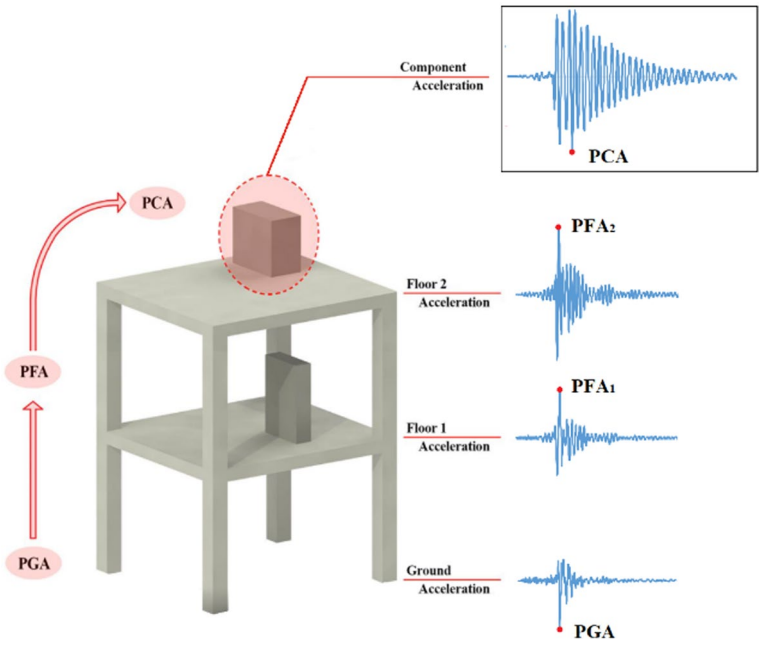

Fig. 1 Amplification of the ground acceleration at the floor and component level [adapted from a presentation in the Working Group 3 of the ATC-120 project by prof. Miranda in 2017]

of the component, both of which can result in resonance if the period of the underlying soil matches the fundamental periods of the structure, or if the component is tuned or nearly tuned to the period of the supporting structure (Goel 2018); the latter is of primary interest here. Knowledge is also required for the component damping level (Kazantzi et al. 2020c), as well as for the position of the component along the building height, since floor and eventually component acceleration demands increase in general with the floor height (NIST 2018). Some design codes treat these amplification sources in a separate manner (e.g., SNZ 2004; ASCE 2017), while others do so simultaneously [e.g., prEN 1998–1-2:2022 (CEN 2022a)]. Irrespectively of this differentiation, all codes seem to adopt a seismic design approach for the nonstructural components that requires the following information (NIST 2017), for which the level of confidence varies:

(a) the design peak ground acceleration (PGA, or in general the design spectrum), which essentially accounts for the seismicity in the region of interest,
(b) an amplification factor that accounts for the increase in the peak floor acceleration (PFA) over the building height relative to the PGA,
(c) an amplification factor that accounts for the increase in the peak component acceleration (PCA) relative to the PFA [in some codes there is no clear distinction between (b) and (c), but rather a single factor is defined to capture both amplification sources],
(d) one or more factors to account for the ductility and overstrength of the nonstructural component and/or of the supporting structure, and
(e) a factor to account for the importance of the nonstructural component or, to put it otherwise, for the severity of the consequences in case the component is damaged.

The provisions of prEN 1998–4:2022 offer three different methods for verifying acceleration-sensitive ancillary elements and their support against the seismic actions. These methods require various levels of data for the supporting structure and the ancillary element. In more detail:

- Method 1 (Sect. 2.1) is presented in Sect. 7 and Annex C of prEN 1998–1-2:2022 (CEN 2022a) and requires for its implementation a high level of knowledge regarding the modal characteristics of the supporting structure (periods of vibration, mode shapes, damping ratios, behaviour factor) and its nested/supported equipment (period of vibration, damping ratio, behaviour factor).
- Method 2 (Sect. 2.2) is the non-dissipative design approach presented in Sect. 9 of prEN 1998–4:2022 (CEN 2022c). The designer is considered to have imperfect knowledge of the modal characteristics of the supporting structure and/or the ancillary element, with the latter assumed to remain essentially elastic during the seismic excitation and (conservatively) have high risk of being tuned to the period of vibration of the supporting structure.
- Method 3 (Sect. 2.3) is the dissipative design approach presented in Sect. 9 of prEN 1998–4:2022 (CEN 2022c), where limited knowledge of the modal characteristics of the structure-element system can be accommodated similarly to Method 2. Certain fuse-like parts of the element's anchorage system are allowed to yield in a ductile manner for energy dissipation. Certified ductility and yielding strength level of said fuses are required.

The engineer is asked to select one of the aforementioned methods to design the anchorage system of an ancillary element. This decision should be based upon two aspects: (a) the level of knowledge and the quality of the available data for the structure-element system dynamic properties, and (b) the type of the element's anchorage system and in particular whether its ductility and overstrength can be certified, allowing a fully dissipative design that limits the acceleration imparted at the component level.

2.1 Method 1—design approach per prEN 1998–1-2:2022

The design horizontal seismic force F_{ap} of an ancillary element residing at floor (or level) j of a structure may be determined after prEN 1998–1-2:2022 (CEN 2022a) as adapted for use in prEN 1998–4:2022 (CEN 2022c):

$$F_{ap} = \frac{\gamma_{ap} \cdot m_{ap} \cdot S_{ap,j}}{q_{ap}'} \tag{1}$$

where γ_{ap} is the performance factor of the element, taking values equal to 1.0 or 1.5 for components non-participating or participating in safety–critical systems, respectively, unless otherwise instructed by a relevant authority or National Annex, m_{ap} is the mass of the ancillary element, q_{ap}' is the period-dependent behaviour factor of the ancillary element, estimated after Annex C of prEN 1998–1-2:2022, but limited to a maximum value of 1.5 per prEN 1998–4:2022 as:

$$q_{ap}' = \min\left(1.5, q_{ap,S} \cdot q_{ap,D}'\right) \tag{2}$$

where $q_{ap,S}$ is the component behaviour factor accounting for all overstrength sources that may be taken equal to 1.3 in the absence of a better-documented value; $q_{ap,D}'$ is a period dependent behaviour factor that accounts for the deformation capacity and the energy dissipation capacity of the component, estimated as:

$$q_{ap,D}' = \begin{cases} 1.0 & T_{ap} \le T_B \\ \text{linear between 1.0 and } q_{ap,D} & T_B \le T_{ap} \le 0.8 \cdot T_{p,1} \\ q_{ap,D} & T_{ap} \ge 0.8 \cdot T_{p,1} \end{cases} \tag{3}$$

$q_{ap,D}$ equals either 1 or 2, for elements not allowed or allowed to dissipate energy via a yielding mechanism, respectively, $T_{p,1}$ is the fundamental period of vibration of the supporting structure, T_B is the lower corner vibration period of the constant spectral acceleration range of the elastic response spectrum after prEN 1998–1-1:2022 (CEN 2022b), and. $S_{ap,j}$ is the value of the floor acceleration spectrum in the considered horizontal direction at floor j, at the natural period of the ancillary element T_{ap} and for a critical damping ratio for the ancillary component of ξ_{ap}.

Finally, if the floor response spectra are not available (e.g., response-history analysis has not been conducted) and the ancillary element cannot be considered as rigid (e.g., it is not a cantilever parapet, sign, billboard, chimney or mast shorter than 4 m), the value of the floor acceleration spectrum $S_{ap,j}$ is evaluated according to the provisions of Annex C. First, this is done separately for each mode of vibration i of the supporting structure as:

$$S_{\mathrm{ap},ij} = \frac{\Gamma_i \cdot \varphi_{ij}}{\left|\left(\frac{T_{\mathrm{ap}}}{T_{\mathrm{p},i}}\right)^2 - 1\right|} \sqrt{\left(\frac{S_{\mathrm{ep},i}}{q_{\mathrm{D}}'}\right)^2 + \left[\left(\frac{T_{\mathrm{ap}}}{T_{\mathrm{p},i}}\right)^2 \cdot S_{\mathrm{eap}}\right]^2} \leq AMP_i \cdot \left|PFA_{ij}\right| \tag{4}$$

where Γ_i is the modal participation factor for the ith mode, which for the direction of interest and given mass m_j at floor/level j, may be evaluated as:

$$\Gamma_i = \frac{\sum m_j \cdot \varphi_{ij}}{\sum m_j \cdot \varphi_{ij}^2} \tag{5}$$

φ_{ij} is the ith mode shape value at the jth floor,

$$AMP_i = \begin{cases} 2.5 \cdot \sqrt{\frac{10}{(5+\xi_{\mathrm{ap}})}}, & \frac{T_{\mathrm{p},i}}{T_{\mathrm{C}}} = 0 \\ \text{linear between } AMP_i\left(\frac{T_{\mathrm{p},i}}{T_{\mathrm{C}}} = 0\right) \text{ and } AMP_i\left(\frac{T_{\mathrm{p},i}}{T_{\mathrm{C}}} = 0.2\right), & 0 \leq \frac{T_{\mathrm{p},i}}{T_{\mathrm{C}}} \leq 0.2 \\ \frac{10}{\sqrt{\xi_{\mathrm{ap}}}}, & \frac{T_{\mathrm{p},i}}{T_{\mathrm{C}}} \geq 0.2 \end{cases} \tag{6}$$

$T_{\mathrm{p},i}$ is the natural period of the i^{th} mode of the supporting (primary) structure, ξ_{ap} is the critical damping ratio (in %) of the ancillary element, PFA_{ij} is the peak floor acceleration in the considered horizontal direction at floor j and for mode i:

$$PFA_{ij} = \Gamma_i \cdot \varphi_{ij} \cdot \frac{S_{\mathrm{ep},i}}{q_{\mathrm{D}}'} \tag{7}$$

$S_{\mathrm{ep},i}$ is the elastic spectral acceleration S_{e} evaluated for the supporting (primary) structure at $T_{\mathrm{p},i}$ and $\xi_{\mathrm{p},i}$, obtained from the elastic response spectrum after prEN 1998–1-1:2022 (CEN 2022b), $\xi_{\mathrm{p},i}$ is the critical damping ratio (in %) of the i^{th} mode of the supporting (primary) structure, equal to 5% (regardless of the lateral-load resisting system) for a building structure,

S_{eap} is the elastic spectral acceleration S_{e} evaluated for the ancillary element at T_{ap} and ξ_{ap}, obtained from the elastic (ground) response spectrum after prEN 1998–1-1:2022 (CEN 2022b), and

q_{D}' is a period-dependent behaviour factor that characterises the primary structure, evaluated as:

$$q_{\mathrm{D}}' = \begin{cases} 1.0 & T_{\mathrm{p},1} \leq T_{\mathrm{A}} \\ \text{linear between 1.0 and } q_{\mathrm{D}} & T_{\mathrm{A}} \leq T_{\mathrm{p},1} \leq T_{\mathrm{C}} \\ q_{\mathrm{D}} & T_{\mathrm{p},1} \geq T_{\mathrm{C}} \end{cases} \tag{8}$$

with T_{A} being the short period cut-off associated to the zero-period spectral acceleration and T_{C} being the upper corner period of the constant spectral acceleration range of the elastic response spectrum of prEN 1988–1-1:2022 (CEN 2022b); q_{D} is the building behaviour factor component accounting for deformation capacity and energy dissipation capacity, as determined by the ductility class considered during the design of the structure, with maximum values provided in the relevant sections of prEN 1998–1-2:2022 (CEN 2022b) for various construction materials and structural systems. For use in industrial structures, a

stricter approach is employed to determine q_D', typically limiting it to 1.0 if no verification of overstrength is undertaken (see Sect. 2.2).

Once the values of $S_{ap,ij}$ are evaluated on the basis of Eq. (4) for all the modes of vibration that contribute significantly to the global response, the value of $S_{ap,j}$ for each floor level j can be computed by combining the pertinent $S_{ap,ij}$. For example, this modal combination can be effected via the square-root-sum-of-squares (SRSS) rule in the case that all modes of vibration (both translational and torsional) are independent from each other. This can be verified by ensuring that

$$\left|T_{p,i} - T_{p,k}\right| / \left(T_{p,i} + T_{p,k}\right) > \xi_{p,i} + \xi_{p,k} \tag{9}$$

for any i and k modes [prEN 1998–1-1:2022 (CEN 2022b)]. Further to the above, at all cases $S_{ap,j}$ should be greater than S_{eap}.

2.2 Method 2—non-dissipative design approach per prEN 1998–4:2022

Industrial facilities are typically subjected to several upgrades during their lifetime, for example, by installing new or replacing old equipment. The anchorage system of such equipment may have to be designed several years after the design and construction of the supporting structure took place. In this context, the implementation of Method 1, which requires a high level of knowledge with regard to the properties of the supporting structure and the nonstructural component, may become a rather daunting task. To work around this actual problem, a second non-dissipative design method (denoted as Method 2 hereinafter) has been adopted in prEN 1998–4:2022 (CEN 2022c).

Given that the relation of the period of the supporting structure with the period of the component is usually unknown, the acceleration applied at the component level, S_{ap} is defined in Method 2 as:

$$S_{ap} = AMP \cdot PFA \tag{10}$$

where AMP is an amplification factor that takes a constant value equal to 7, essentially implying an amplification of the PFA that occurs at a resonance condition between the component and the supporting structure, and.

PFA is the peak floor acceleration corresponding to the fundamental mode of vibration, computed as:

$$PFA = \Gamma_1 \cdot \varphi_{1,ap} \cdot \frac{S_e\left(T_{p,1}, \xi_{p,1}\right)}{q_D'} \geq \frac{S_\alpha}{F_A} \tag{11}$$

where Γ_1 is the participation factor of the fundamental mode in the direction under consideration, which in the absence of more accurate data, can take a value of 1.5 for the majority of the supporting structures, with the exception of tanks and silos where a value of 1.8 is recommended,$\varphi_{1,ap}$ is the fundamental mode shape amplitude at the height z of the supporting structure where the component is attached. If a linear distribution is assumed over the total height H of the supporting structure, then it may be evaluated as $\varphi_{1,ap} = \left(\frac{z}{H}\right)$, with z measured from the ground level,

$S_e(T_{p,1}, \xi_{p,1})$ is the elastic response spectra acceleration at the fundamental period $T_{p,1}$ of the supporting structure in the considered direction and the corresponding damping ratio

$\xi_{p,1}$; the value of $S_e(T_{p,1}, \xi_{p,1})$ employed is subject to a lower bound equal to the elastic response spectra acceleration corresponding to 0.5 s, $S_e(0.5s, \xi_{p,1})$,

S_α is the maximum response spectral acceleration (5% damping) corresponding to the constant acceleration range of the horizontal elastic response spectrum,

F_A is the ratio of the maximum response spectral acceleration (for 5% damping) corresponding to the constant acceleration range of the elastic response spectrum over the zero-period spectral acceleration, often taken equal to 2.5, unless otherwise set by the National Authorities, and $q_D{}'$ is a period-dependent primary-structure behaviour factor (see also Sect. 2.1), evaluated as follows:

(a) For structures with verification that their overstrength does not exceed by more than 20% the design overstrength assumed in code and obtained after prEN 1998–1-1:2022 (CEN 2022b) based on the material and the structural typology, the behaviour factor is computed via Eq. (8).

(b) For structures where there is uncertainty about the q_D value [see Eq. (8)] or no verification of the actual overstrength has been undertaken (which is more likely the case in most practical applications, as this would require detailed nonlinear analysis), then the behaviour factor is:

$$q_D{}' = 1 \tag{12}$$

It should be noted that $q_D{}'$ essentially accounts for the reduction in the seismic forces induced at the component level due to the supporting structure undergoing inelastic deformations prior to the failure of either the ancillary component or its anchorage system. Apparently, estimating the actual overstrength of the supporting structure is a procedure that requires a nonnegligible effort and is also subject to high uncertainty. Further to the above, the industrial assets supporting the ancillary elements are often overdesigned and remain elastic even at high levels of seismic intensity. Thus, a conservative choice, founded on rational evidence, is to disregard the reduction of the induced acceleration demands on the ancillary elements due to the primary structure nonlinearity, i.e., assume that $q_D{}' = 1$.

The design horizontal seismic force F_{ap} of an ancillary element is calculated via Eq. (1), where $S_{ap,j}$ is replaced by S_{ap} after Eq. (10). The period-dependent behaviour factor of the ancillary element, $q_{ap}{}'$, is taken equal to 1.35.

As a final remark, note that Method 2 discards higher mode influence, in the interest of simplifying the process of design when modal information is unavailable. Since resonance can also occur at higher modes of vibration, this could potentially lead to problems for long-period structures, leading to very low values of $S_e(T_{p,1}, \xi_{p,1})$ and thus low *PFA* per Eq. (11). Since most components have periods that are lower than 0.8 s, leading to a non-negligible chance of higher-mode resonance that cannot be conservatively captured, a lower bound of $S_e(0.5s, \xi_{p,1})$ was imposed on the value of $S_e(T_{p,1}, \xi_{p,1})$ that enters Eq. (11).

2.3 Method 3—Dissipative design approach per prEN 1998–4:2022

The code provisions of prEN 1998–4:2022 (CEN 2022c) allow also for a dissipative design approach. Sufficient evidence for the relaxation in the imposed acceleration demands should a yielding element be inserted between a nonstructural component and the supporting system is provided in Kazantzi et al. (2020b, 2022b) and Elkady et al. (2022). Despite its apparent advantages though, this design approach should be used only in cases where

fuse/anchorage systems of verified ductility and strength (guaranteed maximum yielding force) are available. This essentially implies that a yielding fuse of guaranteed/certified ductility and controlled overstrength is installed between the nonstructural component and the supporting structure; all other parts of the load path from floor to component are capacity designed and thus do not fail, resulting in reduced accelerations at the component level and hence protecting the component from damage. In that case, the design horizontal seismic force, F_{ap}, of the fuse may be determined as:

$$F_{ap} = m_{ap} \cdot S_{ap} \tag{13}$$

with S_{ap} computed after Eq. (10). All other elements within the load path from the component to the supporting structure should have at least a 25% overstrength with respect to the fuse strength. In addition, the maximum force (and acceleration) transmitted to the component per Eq. (13), including any fuse overstrength, should not exceed the respective component capacity. The amplification factor *AMP* in Eq. (10) is now evaluated as:

$$AMP = \max\left\{1.30; 0.60 + \frac{1.40}{(\mu_D - 1.0)}\right\} \tag{14}$$

where μ_D is the certified fuse ductility with $\mu_D \geq 1.50$. The cyclic ductility capacity of the fuse should be verified either experimentally by means of cyclic tests or otherwise, and it should be at least equal to $\mu_D \cdot \gamma_{ap}$. In other words, increased performance and safety is served by increasing the ductility capacity, rather than the overstrength of the anchorage system, as the latter would also increase the forces and accelerations transmitted to the component, which is not desirable. Finally, note that the same remarks and remedy made for Method 2 regarding the effect of higher modes also hold here.

3 Case study

An equipment-supporting reinforced concrete (RC) moment resisting frame (Fig. 2), adapted from Kazantzi et al. (2022a), is considered as the case study. This is a typical refinery building, designed for Zone 3 according to the new seismic hazard zonation proposed for Greece by Pitilakis et al. (2022). This essentially corresponds to $S_{\alpha,ref} = 0.71$g for a return period of 475 years, which for the case at hand is amplified by a performance factor of 1.75 as per prEN 1998–4:2022 (CEN 2022c) for Consequence Class 3a (i.e., buildings whose seismic resistance is of importance in view of the consequences associated with collapse) and the Near Collapse (NC) damage state, resulting to $S_{\alpha,ref} = 1.24$g for 2500 years. Detailing compatible with a Ductility Class 2 structure has been assumed, i.e., moderate ductility, in which case the local overstrength capacity, the local deformation capacity, and the local energy dissipation capacity can be taken into account for design. Note that compliance with non-seismic design provisions (especially fire proofing) means such industrial structures are heavily overdesigned, well beyond what seismic loading would require. Hence, no or at worse minor structural damage is anticipated even during strong ground motion shaking events. Thus, an elastic model has been adopted for the supporting structure. In particular, the building was modelled with elastic beam-column elements and a rigid diaphragm was assigned at the floor levels, implying that sufficient in-plane rigidity is guaranteed by the concrete floor slabs. A Rayleigh damping of 5% was assigned to the first two translational modes of vibration.

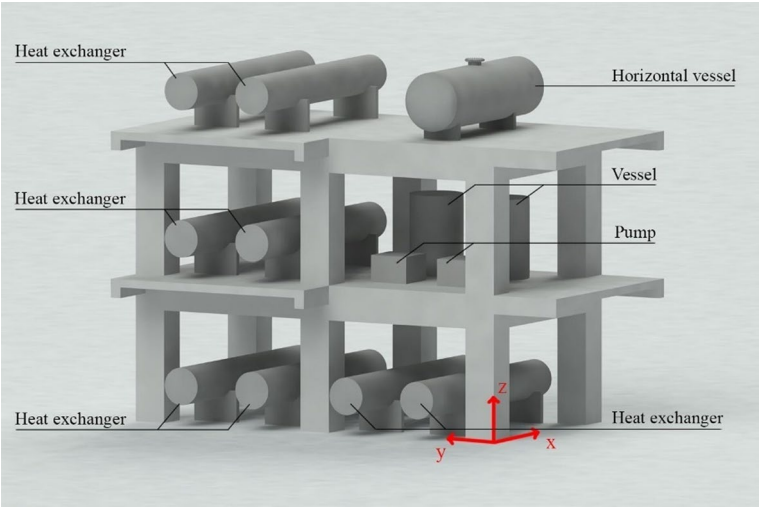

Fig. 2. 3D photorealistic representation of the examined RC building with an example of indicative nested equipment. Equipment at the ground floor is not relevant to this study and only shown for completeness

The anchorage systems of several components nested in the RC building were designed according to the three alternative methods presented in Sect. 2, assuming a performance factor γ_{ap} equal to 1.5 for components participating in safety–critical systems, in order to investigate the level of safety induced by each method; this is undertaken without considering any additional overstrength in the evaluated capacities other than the overstrength that is recommended by the provisions of Eurocode 8, which renders the findings of this study somewhat conservative, yet uniformly so among the different methods. For the investigation, the computed capacities for the acceleration-sensitive ancillary elements were compared to the component acceleration demands at several level of seismic intensity and the probabilities of failure (i.e., of demand exceeding capacity) were then estimated. Both demand and capacity were defined in terms of force for Methods 1 & 2, versus ductility for Method 3. The seismic demands at the component/anchorage level were computed using the floor accelerations that were obtained by means of response-history analyses of the supporting structure. At this point, it should be noted that no collision occurrence was assumed among the equipment, or the equipment and nearby structural elements during the seismic-induced vibration of the building.

A 3D elastic model of the RC building was developed and subjected to a suite of 30 "ordinary" (i.e., non-pulse-like, non-long-duration) natural ground motion records, which were selected by Bakalis et al. (2018) on the basis of the geometric mean of spectra acceleration ordinates between 0.1 s and 1.0 s, $AvgS_a(0.1-1\,\text{s})$. More details on the record selection process can be found in the study of Karaferis et al. (2022). The ground motion spectra of the selected motions are presented in Figs. 3a,b normalized to the same PGA and $AvgS_a(0.1-1\,\text{s})$, respectively.

The floor acceleration histories were recorded at the anchorage points of the nested equipment at both the 1st and the 2nd floor. The equipment was accounted for in the 3D model only via point masses, essentially disregarding any component-structure interaction. This assumption is valid only for components with mass that is not substantial compared to the mass of the supporting structure. The definition of what constitutes a "substantial

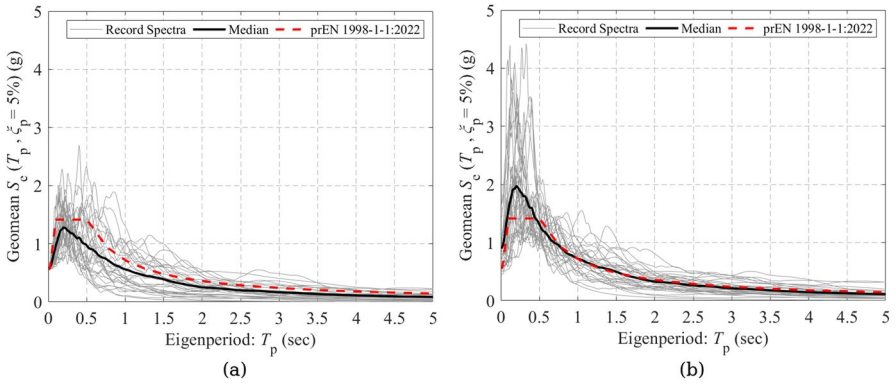

Fig. 3 Ground motion acceleration spectra ($\xi_p = 5\%$) of the 30 selected ground motions scaled to the same level of, **α** S_α/F_A (i.e., equivalent to the PGA in code terms) and **b** $AvgS_a(0.1-1\ s)$, as estimated via the 2% in 50 yrs design spectrum shown in red

mass" varies by large in the pertinent, yet limited literature. ASCE 7–16 (ASCE 2017) sets the limit to 25% of the effective seismic weight of the supporting structure, a condition that was satisfied for the considered supporting structure, and more likely for the majority of the reinforced concrete buildings supporting ordinary industrial equipment. A recent experimental study undertaken within the European H2020 SERA research project on a three-storey industrial steel frame structure with flexible diaphragms supporting four tanks and a cabinet (Butenweg et al. 2021; Nardin et al. 2022) showcased that the effect of the dynamic interaction between the nonstructural components and the primary supporting system is significant for contents with large masses compared to those of the pertinent building. For the case at hand, the seismic weight of the supporting structure is approximately equal to 5600kN whereas the weight of the above ground equipment is about 407kN, which is approximately equal to 7.3% the seismic weight of the building. This ratio is considered quite typical for reinforced concrete equipment supporting buildings, yet it is expected to be higher for steel ones. In the latter case, engineers should check the validity of the cascade method, which allows to decouple the response of the supported equipment from that of the supporting structure. In case that the cascade method conditions are violated, then the dynamic interaction between the supporting building and the nested equipment should be taken into account by means of explicit inclusion of the latter in the model.

Following the computation of the floor acceleration histories at the anchorage points, for each component and in particular for each component-anchorage system, an elastic (Method 1 and Method 2) and an inelastic (Method 3) single degree of freedom (SDOF) system were developed. The inelastic SDOF was assumed to be elastic-perfectly-plastic for the sake of simplicity, considering also different ductility capacity levels. The SDOF systems were subjected to the floor acceleration histories obtained from the previous step (i.e., from the response-history analysis of the entire building) in order to eventually compute the PCA seismic demands.

The building response was assumed to be linear and thus the model for computing the floor acceleration histories was analysed only once for each record at a single intensity level. Then, using the scaling factors obtained from the scaling of the ground acceleration histories on a PGA basis, the results were linearly scaled to account for incrementally increased floor acceleration demands imposed at the anchoring points. A similar process

was extended afterwards to the linear SDOF systems developed for the ancillary components that were designed to remain elastic. In this case, the component acceleration may be evaluated at one level of PFA and then linearly scaled to account for lower or higher floor excitations. Contrarily, evaluating the component acceleration demands for the case of dissipative nonstructural components, i.e., when nonlinear SDOF systems were considered, requires an explicit nonlinear response-history analysis for each one of the considered PFA levels. The main properties of the supporting building along with the installation elevation and type for a set of indicative nested ancillary elements are listed in Table 1.

4 Seismic fragility study

To allow a meaningful comparison of the three different design methodologies that were outlined in Sect. 2, analytical fragility curves for several nested components of varying periods at both floor levels of the case-study building were evaluated. To assess component fragilities, component properties (i.e., yield strength and ductility) were assumed that are close to actual. Specifically, for components designed according to Methods 1 and 2, an overstrength of 1.3 was assumed, as proposed in prEN 1998–1-2:2022 (CEN 2022a) for ancillary components in general. Thus, the design strength was multiplied by 1.3. No added ductility was introduced (i.e., implying a $q_{ap,D} = 1.0$ for Method 1) assuming a failure at the exceedance of the design strength times 1.3. Actually, one may expect the appearance of at least some ductility of the order of 1.1 or 1.2, which will offer some reserve strength. On the other hand, for components designed according to Method 3, yield strength is controlled and overstrength should be limited, as this consequently limits the level of acceleration sustained by the component, which is a design target by itself. Thus, yield strength is assumed to be equal to the design strength. On the other hand, the actual ductility of the component is taken as $\gamma_{ap} \cdot \mu_D$, this being a required property (to be verified by testing) of the fuse per prEN 1998–4:2022 (CEN 2022c). Results are presented for brevity only for the y direction; similar observations hold for the x direction. The comparison of the fragilities essentially allows viewing from a probabilistic standpoint how code-conforming ancillary elements perform if designed on the basis of the three available Eurocode 8 methodologies. The fragility curves have been expressed in terms of the geometric mean PGA as the intensity measure (IM). Other IMs may be more suitable for moderate or long period structures

Table 1 Geometry and properties of the supporting building and the nested equipment with global axis designations per Fig. 2

Floor plan x · y (m^2)	Vibration period of the building $\boldsymbol{T_p}$ (s)	Elevation (m)	Type of ancillary equipment
8.20 · 15.20	$T_{p,1x} = 0.21$ $T_{p,1y} = 0.20$	±0.00	4 × Heat exchanger
		+5.50	2 × Heat exchanger
			2 × Vessel
			2 × Pump
		+11.00	2 × Heat exchanger
			Horizontal vessel

(e.g., O'Reilly and Calvi 2021; Gabbianelli et al. 2022), yet for this short-period two-story building, PGA is good enough for all practical purposes. In particular, parametric models of the component fragility curves were obtained under the typical lognormality assumption (Cornell et al. 2002):

$$P(D > C|PGA = pga) = \Phi\left(\frac{\ln\left(\hat{D}(pga)\right) - \ln\left(\hat{C}\right)}{\beta_{tot}}\right) \tag{15}$$

where $\hat{D}(pga)$ is the median component acceleration demand evaluated for a given $PGA = pga$ level, $\hat{C}$ is the median design acceleration capacity of the component evaluated via one of the three design methodologies, and β_{tot} is the total lognormal dispersion for the PGA level considered. Herein, only demand dispersion was considered, uniformly discarding any capacity variability across all methods. The interested reader may refer to, for instance, Bakalis and Vamvatsikos (2018) and Silva et al. (2019) for more information about the analytical estimation of fragility curves via response history analyses.

4.1 Component fragility for ancillary elements designed to method 1

The design procedure of Method 1 for estimating the design capacity of a component utilises as input several dynamic characteristics (i.e., periods, mode shapes, participation factor, behaviour factors) of both the ancillary elements and the supporting building, as outlined in Sect. 2.1. The most important input elements are the period of the component T_{ap} and the periods of the supporting primary structure $T_{\text{p},i}$. When the former matches any of the latter essentially defines whether the component will be a tuned or untuned one. Method 1 allows for each mode of vibration a maximum amplification of the floor acceleration at the component anchorage level as high as seven (7.07 to be exact, see Fig. 4b) as per Eq. (6) for a component with 2% damping.

As a first test, we assumed perfect knowledge with respect to the periods of structure and component. Specifically, ten (virtual) components with ratios of $T_{\text{ap}}/T_{\text{p,1}}$ within 0.25 to 2.50 were employed. In each case, the component was designed per Method 1 and its

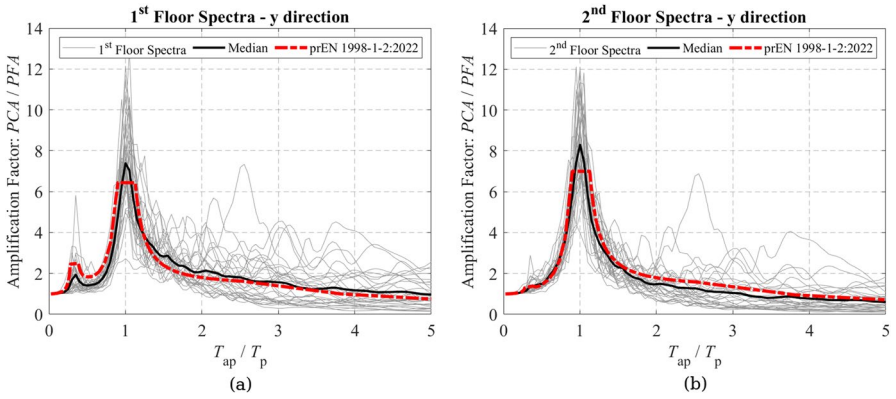

Fig. 4 Floor demand spectra obtained analytically for the y component of the 30 ground motion records showing the amplification factor, which is the ratio of component over floor accelerations at the **a** 1st and **b** 2nd floor levels. The design floor acceleration (capacity) spectrum obtained by means of Method 1 is also presented for comparison

capacity was compared to the elastic floor acceleration spectra derived via (linear) response history analysis. Always, the exact same component period T_{ap} was used to assess demands as well as to determine its capacity, implying a wealth of information on the facility to be constructed and the components to be installed. Thus, any pertinent uncertainties are neglected.

The resulting fragility curves of the (virtual) components in the first and the second floor of the case-study RC building are presented in Fig. 5. Apparently, the most vulnerable component at the top floor is the one tuned to the fundamental period of the supporting structure (see Fig. 5). This outcome was more or less expected, since the generous cut-off limit of seven in the amplification of the design floor spectra implied by Eq. (6), is still exceeded by several records (see Fig. 4), a condition that, for the case at hand, is also reflected in the mean spectrum. It may be argued that such excessive amplification factors are an artefact of the perfectly-elastic response of the structure assumed herein. Yet they have been observed in instrumented conventional buildings during strong ground motions (see Kazantzi et al. 2020a). Regardless, the upper bound amplification employed by the code seems to be a rational compromise that imparts sufficient safety, as even in the rare occurrence of perfect resonance, the component will still be able to sustain moderately higher acceleration demands than those for which it was designed for, due to other additional capacity allowances (e.g., unaccounted ductility). Per Fig. 5, the vast majority of the detuned components have lower probabilities of failure for given PGA values compared to the tuned ones. For the design PGA value of ~0.50g ($\approx 1.75 \cdot 0.28$g), which is obtained from Pitilakis et al. (2022) who defines for Zone 3 a PGA of 0.28 g for a return period of 475 years, a tuned component would have a failure probability as high as ~ 20%. All shorter-period components ($T_{ap}/T_{p,1} < 1$) are considerably safer. Still, a couple of longer-period ones on the 1st floor share the same failure probability with the tuned component, attesting to the mean design spectrum in the tuned region notably being below the actual mean spectrum (and hence imposing less conservatism to the designs) as well as to the high degree of optimisation that went into deriving Method 1. Whether the ~ 20% probabilities of failure are deemed to be safe enough at the design PGA level for a critical facility, is beyond the scope of this manuscript, as any additional reserve capacity is not considered in our assessment. Note also that even though the design PGA corresponds to an intensity level with a mean return period of 2500 years, all three methods essentially scale with the design spectrum, thus similar exceedance probabilities are expected when designing for other return periods.

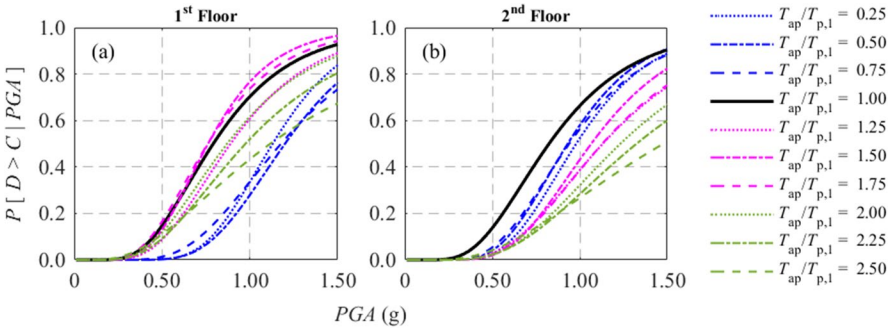

Fig. 5 Component fragility curves computed in the y direction at both building floors, obtained for ancillary elements designed to Method 1 and having ten different period ratios of $T_{ap}/T_{p,1}$

The investigation presented on the failure probability of the components designed to Method 1 was based upon the assumption that the actual (as-built) values of T_{ap} and $T_{p,1}$ are equal to those considered in the design. Nonetheless, this is rarely the case for many different reasons in practical applications. First of all, the anchorage design of the components is usually performed by engineering firms that are different from those that were involved in the design of the supporting structure; in some cases, this means that limited information may be available on the dynamic characteristics of the structure (Kazantzi et al. 2020a). Then, the information regarding the period of the component is also scarce, since manufacturers do not usually provide such data or the ancillary elements may not be anchored to the supporting structure via pre-fabricated connections of known stiffness. It should be pointed out that to regain the aforementioned information (even disregarding any epistemic uncertainties that are always present in analytical studies) is far from trivial, since it requires from the engineer to (a) remodel the supporting structure to obtain its modal characteristics and (b) obtain the fundamental period of the nonstructural component mostly by means of engineering judgement that will be founded on limited (or, at worst, non-existent) literature/experimental evidence.

The practical problems and considerations raised earlier, demonstrate the need to investigate the sensitivity of Method 1 to inaccurate assumptions that could be made during the design process. It is noted that, for simplicity, only the uncertainty due to the period of the component (T_{ap}) is included in the sensitivity analysis. Yet, the findings hold for the case where the uncertainty is associated with the period of the building or both, since we are mostly interested in their relative values rather than their absolute ones. The procedure that was followed involved taking six component $T_{ap,cap}$ over building $T_{p,1}$ period ratios. $T_{ap,cap}$ denotes the assumed periods were employed for evaluating the design component acceleration capacity by means of Method 1. The component acceleration demands were then evaluated assuming that the actual component period (T_{ap}) is different to the one employed for design ($T_{ap,cap}$), being 5/10/20% higher or lower.

The sensitivity analysis results, presented in terms of fragility curves, are illustrated in Fig. 6. It can be inferred that Method 1 can be excessively sensitive to small deviations of the actual period from that assumed in the design. Especially for the case of $T_{ap,cap}/T_{p,1} = 0.75$ (Fig. 6b), where the component is assumed to be detuned during design, small deviations of the actual period from the one assumed could lead to substantially unconservative fragilities. These are much worse than an actually tuned component where no error has taken place in its period estimation ($T_{ap}/T_{ap,cap} = 1.00$), which is denoted by the solid black line. In the worst case of Fig. 6b, where the actual period T_{ap} of the component is 20% higher than the $T_{ap,cap}$ ($T_{ap}/T_{ap,cap} = 1 + 20\%$), the median of the fragility is approximately equal to 0.47 g as opposed to about 0.94 g for $T_{ap}/T_{ap,cap} = 1.00$. Furthermore, for the same case, the failure probability that was estimated for the design PGA at 0.50 g was found to be as high as ~ 55%, which would probably not be acceptable for critical facilities. Similar safety problems ensue for a high initial estimate of the component period at $T_{ap,cap}/T_{p,1} = 1.25$ (Fig. 6d) and an estimation error in the opposite direction ($T_{ap}/T_{ap,cap} = 1 - 20\%$). Concluding, it could be said that Method 1 works consistently well when the designer has a good level of knowledge about the actual periods of the component and the supporting structure, but it is likely to render unconservative designs in several cases if the periods of the component and/or the structure deviate from the actual values in a way that brings them closer to tuning when originally no resonance was assumed.

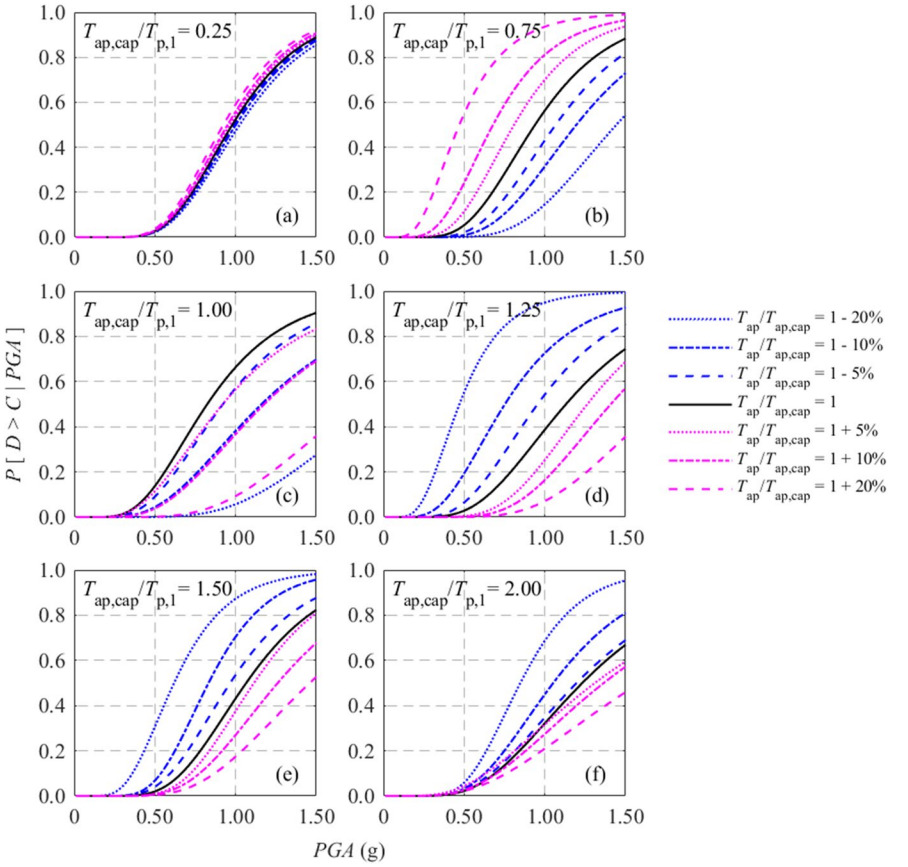

Fig. 6 Fragility-based sensitivity analysis for components designed per Method 1, presented indicatively for the 2nd Floor

4.2 Component fragility for ancillary elements designed to method 2

To remove the uncertainty associated with the assumptions made for the design periods of the component and the supporting building, one may adopt Method 2 (presented in Sect. 2.2); this can arrest the propagation of uncertainty associated with the vibration periods from the design level to the fragilities of the ancillary elements. Method 2 is essentially a simpler version of Method 1 for non-dissipative design, where the design component acceleration (design PCA) is always computed on the basis of resonance. Thus, a maximum amplification factor of $AMP = 7$ is adopted, which approximately corresponds to the maximum AMP applied at the floor acceleration of Method 1 for components having a damping of 2%. The corresponding fragilities for components designed to Method 2 for both building floors are presented in Fig. 7. It should be noted that the PFA in Method 2 was evaluated herein considering the actual mode shape of the first mode, likewise Method 1, rather than adopting a simple linear modal shape. Later in the manuscript the implications of this decision will be further investigated.

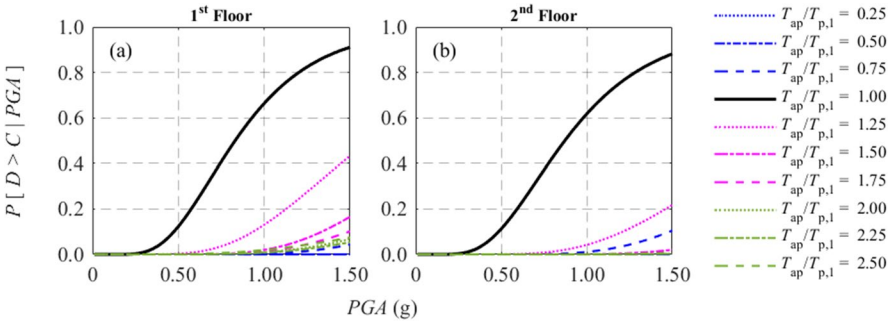

Fig. 7 Component fragility curves computed in the y direction for both building floors, obtained for ancillary elements designed to Method 2

Evidently, the most fragile components are those tuned to the predominant vibration period of the supporting building ($T_{ap}/T_{p,1} = 1.00$), achieving a near-identical performance to Method 1 (see Table 2) when there is no uncertainty about periods (Fig. 5). The apparent advantage of this method is that it guarantees consistently conservative designs for all components, regardless of period; however, this comes with some non-negligible overdesign for detuned components. If one considers that the cost of even a heavily overdesigned anchorage system is trivial compared to the overall value of a critical facility, its functionality and safety, then Method 2 offers some considerable advantages to practical design: By virtue of being period-agnostic, it nullifies by default any bias associated with the period estimation for both the component and the supporting building.

4.3 Component fragility for ancillary elements designed to method 3

Method 3 (Sect. 2.3) goes one step beyond Method 2, aiming to alleviate its conservatism associated with designing a nonstructural component as potentially tuned to the period of the supporting building. This is achieved by introducing a fuse of guaranteed ductility and

Table 2 Median and dispersion of the component fragility curves for the 1st floor in the y direction of the case study building as obtained from the three Eurocode 8 design methods

$T_{an}/T_{p,1}$	Method 1		Method 2		Method 3 $\mu_D = 1.5$		Method 3 $\mu_D = 2.0$		Method 3 $\mu_D = 2.5$		Method 3 $\mu_D = 3.0$	
	μ	σ	μ	σ	μ	σ	μ	σ	μ	σ	μ	σ
0.25	1.13	0.29	4.83	0.29	3.65	0.35	2.86	0.35	2.74	0.35	2.79	0.35
0.50	1.20	0.31	4.23	0.31	1.99	0.34	1.25	0.35	1.01	0.36	0.90	0.36
0.75	1.18	0.39	2.91	0.39	1.59	0.38	1.09	0.37	0.94	0.36	0.89	0.35
1.00	0.79	0.44	0.83	0.44	1.25	0.42	1.00	0.39	0.96	0.39	0.96	0.40
1.25	0.89	0.42	1.61	0.42	1.64	0.43	1.30	0.40	1.22	0.39	1.20	0.39
1.50	0.76	0.37	2.16	0.37	1.99	0.42	1.52	0.42	1.43	0.44	1.42	0.45
1.75	0.76	0.43	2.59	0.43	2.13	0.45	1.73	0.50	1.63	0.50	1.65	0.59
2.00	0.87	0.47	3.01	0.47	2.65	0.53	2.12	0.57	1.99	0.55	1.97	0.56
2.25	0.98	0.50	3.36	0.50	3.12	0.61	2.53	0.58	2.31	0.58	2.40	0.62
2.50	1.12	0.65	3.85	0.65	3.47	0.66	2.74	0.71	2.62	0.62	2.54	0.64

strength in the load path, thus removing the effect of resonance and tying the amplification factor of the peak floor acceleration to the yielding fuse ductility [see Eq. (14)]. This sacrificial fuse is essentially an element of the anchorage system, explicitly designed and verified to develop a controlled yielding mechanism should the seismic force (or acceleration) exceed a predetermined level. The end effect of allowing the fuse to undergo inelastic deformation is the substantial reduction of the accelerations that are imparted to the component, even under the persistent design condition that the component is tuned. In fact, as it was showcased analytically by Kazantzi et al. (2020a; b; 2022b) and experimentally by Elkady et al. (2022), if nonlinearity is permitted at the component level, the strong narrowband amplification effect is substantially limited, even in the vicinity of the tuning range and even for small inelastic displacements.

Figure 8 illustrates the component fragility curves that were obtained by having the component capacities evaluated via Method 3, considering four fuse ductility levels, i.e., $\mu_D = \{1.5;2.0;2.5;3.0\}$. Note that such values are only nominal, meant to be used for determining AMP per Eq. (14), with actual ductilities being $\gamma_{ap} = 1.5$ times higher per the design requirements of the case study. As can be inferred by inspecting Fig. 8 (and Table 2), Method 3 yields component fragilities that are slightly safer than those of Methods 1 and 2 at resonance, yet of considerably more reasonable (i.e., lesser) conservatism for detuned components when compared to the ultra-conservative Method 2. Moreover, it offers one less obvious but equally important advantage: Components designed by Method 3 eventually sustain considerably lower accelerations, limited by the fuse yield strength. In other words, by virtue of exploiting the detuning effect of hysteresis, even nominally resonant components receive PFA amplification factors much lower than 7. Thus, not only component safety but also functionality can be secured. Notably, providing a fuse of increased μ_D is not meant to decrease the failure probability per se (see Fig. 7), but to decrease the forces and accelerations that the component sustains while maintaining

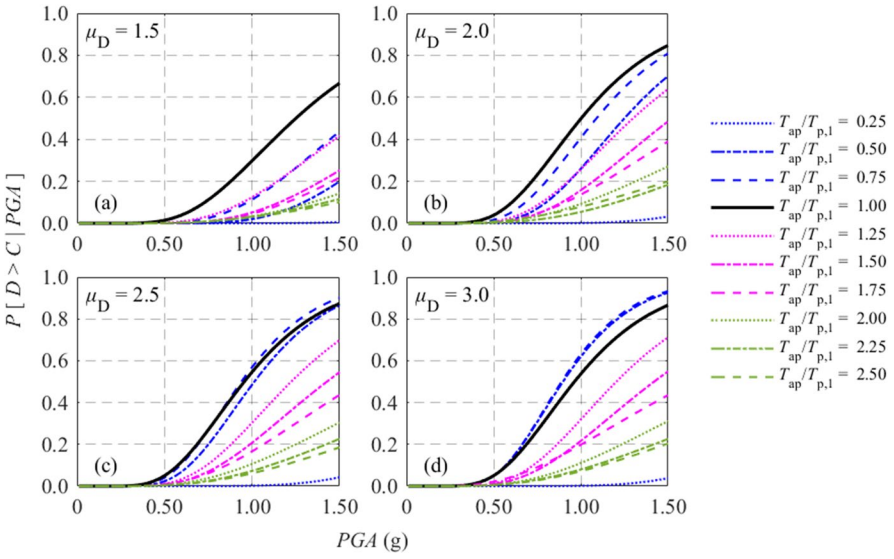

Fig. 8 Component fragility curves computed for the critical 1st Floor in the y direction, obtained for ancillary elements designed to Method 3. Note that the nominal ductility capacity μ_D is reported in the legend, whereas the actual ductility capacity is $1.5 \cdot \mu_D$

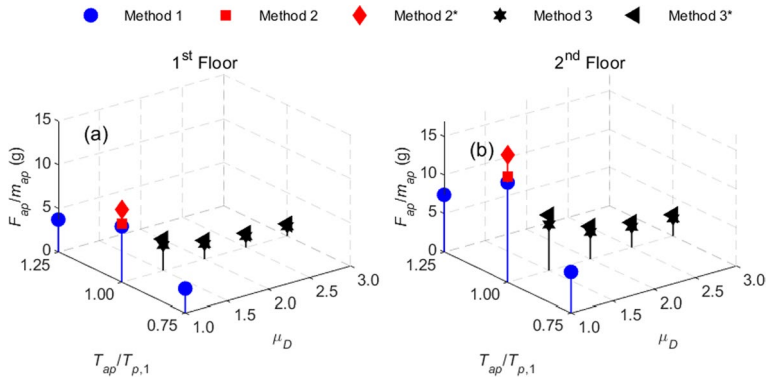

Fig. 9 Component acceleration capacities as obtained for the three Eurocode 8 component design methodologies for, **a** the 1st and **b** the 2nd Floor. The '*' superscript denotes a simplified version of Methods 2 and 3 where approximated rather than actual modal properties are considered for the supporting structure

similar safety levels. Thus, the amplification per Eq. (14) starts at $AMP = 3.4$ for $\mu_D = 1.5$, then drops to $AMP = 2.0$ for $\mu_D = 2.0$, and levels off at $AMP = 1.3$ for $\mu_D = 3.0$. At this point, it should be mentioned that Method 1 also has a provision [via the period dependent behaviour factor $q_{ap,D}'$ of Eq. (3)] to account for the energy dissipation due to the potential inelastic seismic response of the component. Yet, this provision offers a generic and non-guaranteed mitigation of the component acceleration demands due to the yielding of the component, contrary to Method 3 that sets strict criteria on what constitutes an acceptable dissipative mechanism. Indicative medians (μ) and dispersions (σ) of the component fragilities obtained from the three Eurocode 8 design approaches are summarised in Table 2.

The design component acceleration capacities F_{ap}/m_{ap} that are evaluated from each one of the presented Eurocode 8 design approaches are presented in Fig. 9 to offer a quantitative overview and comparison. Therein, two-versions of Methods 2 and 3 are shown, namely Methods 2* and 3*, where the '*' superscript denotes the use of approximated modal properties of $\Gamma_1 = 1.5$ and linear fundamental modal shape $\varphi_{1,ap}$, rather than actual modal properties For brevity, only salient values are shown in Fig. 9. Hence, for Methods 2 and 2* only one value is presented since irrespectively of the period ratio and the ductility level they yield the same component acceleration capacity estimates. Similarly, Methods 3 and 3* are independent of the period ratio and indicative results are presented only for the tuned case.

As evident, Methods 3 and 3* yield the lowest design acceleration capacities for the considered period ranges, i.e., $T_{ap}/T_{p,1} = \{0.75;1.00;1.25\}$. For instance, a design by Method 3 yields irrespectively of the $T_{ap}/T_{p,1}$ ratio an acceleration capacity that is about 57% lower for a component ductility of 1.5 and 74% lower for a component ductility of 2.0 than that of Method 2 for the critical 1st Floor. Moreover, Method 3, despite the fact that it is founded upon the conservative assumption that the component is always tuned, yields also lower component acceleration requirements compared to Method 1 not only for the tuned components but also for the components that are in the vicinity of the tuning region (expect for the lowest ductility in the case of $T_{ap}/T_{p,1} = 0.75$). Due to the capping in the allowable AMP factor, no additional reduction in the acceleration capacity requirements is manifested beyond a ductility of 3.0. Finally, note that for period ranges far from any tuning, i.e. either much shorter or longer than the ones shown in Fig. 9, the accurate floor

spectrum employed by Method 1 is expected to provide lower design accelerations compared to all other candidates.

Summing up, one should not try to generalise these findings beyond low-rise structures with minimal higher mode influence. Given the simplifications introduced in Methods 2 and 3, whereby higher modes are neglected and their influence is accounted for only approximately by introducing a lower bound on the peak floor acceleration, one cannot have the full picture of how Methods 1 to 3 fare for mid-rise or high-rise cases. Still, we can say with some conviction that when base isolation is not an option, then for vibration-sensitive equipment, which is likely to be damaged prior to its anchorage system due to the excessive acceleration demands, Method 3 is certainly preferable to the other two alternatives, irrespectively of the state of knowledge about the dynamic properties of the component and the supporting structure. The only missing link for the widespread application of Method 3 is the limited availability of anchoring products with verified ductility and strength. Nevertheless, this is an issue to be resolved by manufactures who wish to offer products of superior and guaranteed seismic performance. Otherwise, Methods 1 and 2 are the only alternatives.

5 Conclusions

A comparison study was undertaken to investigate the seismic performance of ancillary elements in industrial facilities that are designed according to the regulations prescribed by the three design routes offered in the 2022 revised version of Eurocode 8. The study explicitly accounted for the level of knowledge that is needed to apply each one of these design methodologies and explored how the uncertainties associated with the required input propagate to the final design. It was showcased by means of an analytical seismic fragility assessment that the design method in Eurocode 8—Part 1–2 (prEN 1998–1-2:2022) can deliver robust designs in those cases where the designer has a high level of knowledge with regards to the dynamic properties of the supporting structure and the nonstructural component. These properties may refer to the vibration periods of the latter (explicitly investigated in this study) or to other characteristics that may be difficult to accurately estimate for a number of structures, e.g. the mode shapes or the damping level. However, if such a high level of knowledge is not the case, it was demonstrated that even small discrepancies of the assumed properties from their actual values can severely undermine the seismic reliability of an otherwise well-designed code-conforming nonstructural element. Contrariwise, the design methodologies offered in Eurocode 8 – Part 4 (prEN 1998–4:2022) are less sensitive to uncertainty in the properties of the supporting structure and the ancillary elements and hence deliver design products that possess seismic performance that is consistently superior to that of the component that has its vibration period tuned to the period of the supporting structure. If a non-dissipative approach is taken, then this is achieved by sheer abundance of overstrength. If instead one employs a dissipative fuse of verified strength and ductility as part of the anchorage system, then substantially lower component acceleration demands are obtained. This latter property is of interest to engineers appointed to design the anchorage systems for vibration-sensitive equipment.

Acknowledgements The authors acknowledge the support of CEN TC250/SC8/PT5 team in charge of EN 1998-4, namely Drs. C. Butenweg, C. Fernandez, R. Nascimbene, and C. Rebelo, as well as Drs. P. Bisch, and A. Correira of TC250/SC8. Thanks go to Ms. E. Vourlakou for preparing the building images. We also

acknowledge the comments made by the three anonymous reviewers who helped us improve the overall quality of this manuscript.

Funding Open access funding provided by HEAL-Link Greece. This research has been co-financed by the European Union through the HORIZON2020 research and innovation programme "METIS–Seismic Risk Assessment for Nuclear Safety" under Grant Agreement No. 945121 and the HORIZON-EUROPE innovation action "PLOTO–Deployment and Assessment of Predictive modelling, environmentally sustainable and emerging digital technologies and tools for improving the resilience of IWW against Climate change and other extremes" under Grant Agreement No. 101069941.

Data availability Some or all data, models, or code that support the findings of this study are available from the corresponding author upon reasonable request.

Declarations

Competing interests The authors have no relevant financial or non-financial interests to disclose.

References

Adam C, Fotiu PA (2000) Dynamic analysis of inelastic primary secondary systems. Eng Struct 22(1):58–71. https://doi.org/10.1016/S0141-0296(98)00073-X

ASCE (2017) Minimum design loads and associated criteria for buildings and other structures. ASCE/SEI 7-16, American Society of Civil Engineers, Virginia. https://doi.org/10.1061/9780784414248

Bakalis K, Vamvatsikos D (2018) Seismic fragility functions via nonlinear response history analysis. J Struct Eng (ASCE) 144(10):04018181. https://doi.org/10.1061/(ASCE)ST.1943-541X.0002141

Bakalis K, Kohrangi M, Vamvatsikos D (2018) Seismic intensity measures for above-ground liquid storage tanks. Earthq Eng Struct Dynam 47(9):1844–1863. https://doi.org/10.1002/eqe.3043

Butenweg C, Bursi OS, Paolacci F, Marinkovic M, Lanese I, Nardin C, Quinci G (2021) Seismic performance of an industrial multi-storey frame structure with process equipment subjected to shake table testing. Eng Struct 243:112681. https://doi.org/10.1016/j.engstruct.2021.112681

CEN (2022a) Eurocode 8: — Design of structures for earthquake resistance—part 1–2: Rules for new buildings. prEN 1998–1–2:2020

CEN (2022b) Eurocode 8: — Design of structures for earthquake resistance—part 1–1: General rules and seismic action. prEN 1998–1–1:2021

CEN (2022c) Eurocode 8: — Design of structures for earthquake resistance—part 4: Silos, tanks and pipelines, towers, masts and chimneys. prEN 1998–4:2021

Cornell CA, Jalayer F, Hamburger RO, Foutch DA (2002) The probabilistic basis for the 2000 SAC/ FEMA steel moment frame guidelines. J Struct Eng (ASCE) 128(4):526–533. https://doi.org/10.1061/(ASCE)0733-9445(2002)128:4(526)

Elkady A, Vamvatsikos D, Lignos D, Kazantzi AK, Miranda E (2022) Experimental studies to validate an improved approach to the design of acceleration-sensitive nonstructural elements. In: Fifth international workshop on the seismic performance of non-structural elements (SPONSE), Palo Alto, California (USA)

FEMA, HAZUS Earthquake Model Technical Manual (2020) https://www.fema.gov/sites/default/files/2020-10/fema_hazus_earthquake_technical_manual_4-2.pdf

Gabbianelli G, Perrone D, Brunesi E, Monteiro R (2022) Seismic acceleration demand and fragility assessment of storage tanks installed in industrial steel moment-resisting frame structures. Soil Dyn Earthq Eng 152:107016. https://doi.org/10.1016/j.soildyn.2021.107016

Gandelli E, Taras A, Distl J, Quaglini V (2019) Seismic retrofit of hospitals by means of hysteretic braces: Influence on acceleration-sensitive non-structural components. Front Built Environ 5:100. https://doi.org/10.3389/fbuil.2019.00100

Goel RK (2018) Seismic forces in ancillary components supported on piers and wharves. Earthq Spectra 34(2):741–758. https://doi.org/10.1193/041017EQS068M

Igusa T, Der Kiureghian A (1985) Generation of floor response spectra including oscillator-structure interaction. Earthquake Eng Struct Dynam 13(5):661–676. https://doi.org/10.1002/eqe.4290130508

Karaferis ND, Kazantzi AK, Melissianos VE, Bakalis K, Vamvatsikos D (2022) Seismic fragility assessment of high-rise stacks in oil refineries. Bull Earthq Eng 20:6853–6876. https://doi.org/10.1007/s10518-022-01472-2

Kazantzi AK, Vamvatsikos D, Miranda E (2020a) Evaluation of seismic acceleration demands on building non-structural elements. J Struct Eng (ASCE) 146(7):04020118. https://doi.org/10.1061/(ASCE)ST.1943-541X.0002676

Kazantzi AK, Miranda E, Vamvatsikos D (2020b) Strength-reduction factors for the design of light non-structural elements in buildings. Earthq Eng Struct Dynam 49(13):1329–1343. https://doi.org/10.1002/eqe.3292

Kazantzi AK, Vamvatsikos D, Miranda E (2020c) The effect of damping on floor spectral accelerations as inferred from instrumented buildings. Bull Earthq Eng 18:2149–2164. https://doi.org/10.1007/s10518-019-00781-3

Kazantzi AK, Karaferis ND, Melissianos VE, Bakalis K, Vamvatsikos D (2022a) Seismic fragility assessment of building-type structures in oil refineries. Bull Earthq Eng 20:6877–6900. https://doi.org/10.1007/s10518-022-01476-y

Kazantzi AK, Miranda E, Vamvatsikos D, Elkady A, Lignos D (2022b) Analytical studies in support of an improved approach to the design of acceleration-sensitive nonstructural elements. In: Fifth international workshop on the seismic performance of non-structural elements (SPONSE), Palo Alto, California (USA)

Lee JP, Chen C (1975) Vertical responses of nuclear power plant structures subject to seismic ground motions. In: 3rd SMiRT conference, London, United Kingdom, Paper K5/3. https://repository.lib.ncsu.edu/bitstream/handle/1840.20/28385/K5-3.pdf?sequence=1

Merino Vela RJ, Brunesi E, Nascimbene R (2019) Seismic assessment of an industrial frame-tank system: development of fragility functions. Bull Earthq Eng 17:2569–2602. https://doi.org/10.1007/s10518-018-00548-2

Miranda E, Kazantzi AK, Vamvatsikos D (2018) New approach to the design of acceleration-sensitive non-structural elements in buildings. In: 16th European conference on earthquake engineering, Thessaloniki, Greece. http://papers.16ecee.org/files/805%20MirandaKazantziVamvatsikos.pdf

Nardin C, Bursi OS, Paolacci F, Pavese A, Quinci G (2022) Experimental performance of multi-storey braced frame structure with non-structural industrial components subjected to synthetics ground motions. Earthquake Eng Struct Dynam 51(9):2113–2136. https://doi.org/10.1002/eqe.3656

NIST (2017) Seismic analysis, design and installation of nonstructural components and systems background and recommendation for future work. Prepared by the Applied Technology Council for the US National Institute of Standards and Technology, Gaithersburg

NIST (2018) Recommendations for improved seismic performance of nonstructural components. Prepared by the Applied Technology Council for the U.S. National Institute of Standards and Technology, Gaithersburg, MD, https://doi.org/10.6028/NIST.GCR.18-917-43

O'Reilly GJ, Calvi GM (2021) A seismic risk classification framework for non-structural elements. Bull Earthq Eng 19(13):5471–5494. https://doi.org/10.1007/s10518-021-01177-y

Peters KA, Schmitz D, Wagner U (1977) Determination of floor response spectra on the basis of the response spectrum method. Nucl Eng Des 44(2):255–262. https://doi.org/10.1016/0029-5493(77)90032-2

Pinkawa M, Vulcu C, Hoffmeister B (2022) Seismic performance of industrial components supporting steel structures—Past damages, current design practice and recent experimental tests. In: Mazzolani FM, Dubina D, Stratan A (Eds). In: Proceedings of the 10th international conference on behaviour of steel structures in seismic areas (STESSA), Lecture Notes in Civil Engineering 262:535–543. https://doi.org/10.1007/978-3-031-03811-2_56

Pitilakis K, Riga E, Apostolaki S (2022) Proposal for a new seismic hazard zonation map for Greece. In: 3rd European conference on earthquake engineering & seismology, Bucharest, Romania

Sankaranarayanan R, Medina RA (2007) Acceleration response modification factors for nonstructural components attached to inelastic moment-resisting frame structures. Earthquake Eng Struct Dynam 36(14):2189–2210. https://doi.org/10.1002/eqe.724

Silva V, Akkar S, Baker J, Bazzurro P, Castro JM, Crowley H, Dolsek M, Galasso C, Lagomarsino S, Monteiro R, Perrone D, Pitilakis K, Vamvatsikos D (2019) Current challenges and future trends in analytical fragility and vulnerability modeling. Earthq Spectra 35(4):1927–1952. https://doi.org/10.1193/042418EQS101O

Singh MP (1980) Seismic design input for secondary systems. J Struct Div 106(2):505–517. https://doi.org/10.1061/JSDEAG.0005371

SNZ (2004) Structural design actions—part 5: earthquake actions—New Zealand. NZ1170.5, Standards New Zealand, Wellington, New Zealand. https://www.standards.govt.nz/shop/nzs-1170-52004/

Taghavi S, Miranda E (2003) Response assessment of nonstructural building elements, PEER Report 2003/05. https://peer.berkeley.edu/sites/default/files/0305_s._taghavi_e._miranda_.pdf

Taghavi S, Miranda E (2008) Effect of interaction between primary and secondary systems on floor response spectra. In: The 14th world conference on earthquake engineering, Beijing, China

Vukobratovic V, Ruggieri S (2021) Floor acceleration demands in a twelve-storey RC shear wall building. Buildings 11(2):38. https://doi.org/10.3390/buildings11020038

Wang S, Yang Y, Lin F, Jeng J, Hwang J (2017) Experimental study on seismic performance of mechanical/electrical equipment with vibration isolation systems. J Earthq Eng 21(3):439–460. https://doi.org/10.1080/13632469.2016.1172374